Impact of Nonischemic Scar Features on Local Ventricular Electrograms and Scar-Related Ventricular Tachycardia Circuits in Patients with Nonischemic Cardiomyopathy

Takeshi Sasaki, MD, PhD[1], **Christopher F. Miller, MS**[1], **Rozann Hansford, RN, MPH**[1], **Vadim Zipunnikov, PhD**[2], **Menekhem M. Zviman, PhD**[1], **Joseph E. Marine, MD**[1], **David Spragg, MD**[1], **Alan Cheng, MD**[1], **Harikrishna Tandri, MD**[1], **Sunil Sinha, MD**[1], **Aravindan Kolandaivelu, MD**[1], **Stefan L. Zimmerman, MD**[3], **David A. Bluemke, MD, PhD**[4], **Gordon F. Tomaselli, MD**[1], **Ronald D. Berger, MD, PhD**[1], **Henry R. Halperin, MD**[1], **Hugh Calkins, MD**[1], and **Saman Nazarian, MD, PhD**[1]

[1]Department of Cardiology, Johns Hopkins University, Baltimore

[2]Department of Biostatistics, Johns Hopkins University, Baltimore

[3]Department of Radiology, Johns Hopkins University, Baltimore

[4]Radiology and Imaging Sciences, NIH Clinical Center, National Institute of Biomedical Imaging and Bioengineering, Bethesda, MD

Abstract

Background—The association of local electrogram features with scar morphology and distribution in nonischemic cardiomyopathy (NICM) has not been investigated. We aimed to quantify the association of scar on late-gadolinium enhanced cardiac magnetic resonance (LGE-CMR) with local electrograms and ventricular tachycardia (VT) circuit sites in patients with NICM.

Methods and Results—Fifteen patients with NICM underwent LGE-CMR before VT ablation. The transmural extent and intramural types (endocardial, mid-wall, epicardial, patchy, transmural) of scar were measured in LGE-CMR short axis planes. Electro-anatomic map (EAM) points were registered to LGE-CMR images. Myocardial wall thickness, scar transmurality, and intramural scar types were independently associated with electrogram amplitude, duration, and deflections in linear mixed effects multivariable models, clustered by patient. Fractionated and isolated potentials were more likely to be observed in regions with higher scar transmurality (P<0.0001 by ANOVA) and in regions with patchy scar (versus endocardial, mid wall, epicardial scar, P<0.05 by ANOVA). Most VT circuit sites were located in scar with >25% scar transmurality.

Conclusions—Electrogram features are associated with scar morphology and distribution in patients with NICM. Prior knowledge of electrogram image associations may optimize procedural strategies including the decision to obtain epicardial access.

Correspondence: Takeshi Sasaki, MD, Division of Cardiology, Johns Hopkins University, Carnegie 592A, 600 N. Wolfe Street, Baltimore, MD 21287, Tel: 410-614-2751, Fax: 410-502-4854, tsasaki.cvm@tmd.ac.jp.

Keywords

ventricular tachycardia; nonischemic cardiomiopathy; cardiac magnetic resonance imaging; electrophysiology mapping

Introduction

Catheter ablation is often used as an adjunct to implantable cardioverter defibrillators (ICD) and medical therapy for management of scar-related ventricular tachycardia (VT) in patients with ischemic[1–8] and nonischemic cardiomyopathy (NICM).[8–18] However, an endocardial ablation strategy is sometimes limited due to the propensity for epicardial, mid wall, and patchy scar morphologies characteristic of NICM.[19] Epicardial ablation has improved ablation outcomes for scar-related VTs in patients with failed endocardial ablation and an epicardial substrate.[8–12] However, even with epicardial mapping, mid wall scar may not be identified using voltage mapping and thresholds defined based on data from ischemic substrates. Endocardial unipolar voltage mapping may detect mid wall and epicardial nonischemic scar,[11,17] albeit with lower specificity. Characterization of the nonischemic VT substrate by LGE-CMR, may lead to optimization of electrogram (EGM) thresholds for identification of midwall and epicardial scar and enable pre-procedural planning for epicardial access. We sought to quantify associations between scar characteristics on LGE-CMR, and EGM features and VT circuit sites on endocardial EAM, to gain insights regarding the nonischemic substrate for VT.

Methods

Study patients

Our Institutional Review Board approved the study protocol. All patients provided written informed consent. We enrolled 15 consecutive patients with monomorphic VT and NICM that consented to undergoing MRI prior to VT ablation. Patients with hypertrophic cardiomyopathy, arrhythmogenic right ventricular dysplasia, and renal dysfunction (glomerular filtration rate < 60 ml/min/1.73m^2) were excluded.

CMR studies

CMR was performed with a 1.5T CMR scanner (Avanto, Siemens, Erlangen, Germany). In 13 patients with ICD systems, potential risks were explained and CMR images were obtained using our established safety protocol.[20] Short axis spoiled gradient echo cine images were acquired with repetition time (TR) 40 ms; echo time (TE) 3.1 ms; flip angle 15°, average in plane resolution 2.0×1.6 mm; slice thickness 6 mm. Next, 0.2 mmol/kg intravenous gadopentetate dimeglumine was administrated and MR angiography images were acquired with TR 2.9 ms; TE 1.08 ms; flip angle 25°, average in-plane resolution 1.0×1.0 mm, slice thickness 1.0 mm. Ten minutes after the injection of the contrast medium, LGE-CMR images were obtained in short axis with a segmented inversion-recovery gradient-echo turbo fast low angle shot sequence (TR 1 R-R interval; TE 1.04 ms; flip angle 25°, average in-plane resolution 1.3×1.3 mm; slice thickness, 8 mm; and inversion time typically 240–360 ms). The inversion time was modified iteratively to obtain maximal nulling of the signal from normal ventricular myocardium.

CMR Image Analysis

QMass MR software (Medis, Leiden, Netherlands) was used to measure scar transmurality and LV wall thickness in short axis image planes that did not include the mitral annulus. Candidate hyperenhanced regions were identified as scar if the mean intensity of the

hyperenhanced region was >6 standard deviations above the mean intensity of remote normal myocardium.[21,22] Scar transmurality and left ventricular (LV) wall thickness were determined as previously described.[4,16] Intramural scar types were recorded based on the classification of NICM scar in previous reports (endocardial, mid wall, epicardial, patchy, transmural scar; Figure 1A).[19] In contrast to the other scar types which exhibited cohesive areas of fibrosis, patchy scar regions were inhomogeneous with alternating areas of scar and viable tissue in close proximity and extending from endocardium to epicardium (Figure 1A).

Electrophysiological Study

In patients with ICD systems, tachyarrhythmia therapies were disabled prior to the procedure. Ventricular programmed-stimulation to induce VT was performed using a quadripolar catheter at the right ventricular (RV) apex and outflow tract with up to triple extrastimuli at three basic cycle lengths. If the induced VT sustained without hemodynamic collapse, EAM was attempted during the tachycardia. Otherwise, substrate mapping was performed during sinus rhythm or back-up ventricular pacing.

3-dimensional Electroanatomic Maps and Electrogram Characteristics

A 3-dimensional EAM system (CARTO, Biosense Webster, Inc., Diamond Bar, CA) was used to create endocardial voltage maps in LV and/or RV during sinus rhythm or back-up ventricular pacing using a 3.5 mm-tip electrode with 2 mm inter-electrode spacing (Thermocool, Biosense Webster, Inc.) and "Fill Threshold" set at 15mm. After administration of sufficient heparin to maintain an activated clotting time of >300 seconds, the mapping catheter was inserted into the LV using a transseptal approach. The LV and/or RV shell reconstructed from the CMR angiogram was registered to the LV and/or RV EAMs using the landmark registration method as previously described.[4] Registration accuracy was determined using statistical summation, which is the average distance of each EAM point to the closest surface point of the reconstructed image of the chamber. Local EGM bipolar and unipolar voltage, duration and deflection were measured (Figure 1B).[4,16, 23] Electroanatomic mapping was performed during sinus rhythm in all patients except one patient with complete heart block, in whom mapping was performed during right ventricular pacing. Bipolar and unipolar EGMs were filtered at 10–400Hz and 1–240Hz, respectively, and recorded as the difference between the highest and lowest deflections of a stable contact signal. EGM duration and deflection were measured from the onset to the end of the EGM deflections at 400mm/s speed manually. The number of deflections was counted as the summation of both negative and positive deflections in each EGM. Fractionated potentials and isolated potentials on bipolar EGMs were identified based upon previously published criteria: fractionated: voltage 0.5mV, duration 133ms, and/or amplitude/duration ratio <0.005, isolated potential: a potential separated from the ventricular EGM by an isoelectric segment, and/or a segment with low voltage noise (<0.05 mV) of >20 msec duration at a gain of 40–80 mm/mV.[4,24] Two independent observers analyzed EGM characteristics. Discrepancies were resolved by repeat review by a third observer and consensus among all reviewers. In accepting the EGM in each EAM point, we confirmed that at least 2 consecutive EGMs had the same morphology to avoid EGM artifact due to poor catheter contact.

Catheter Ablation of Scar-related VT

Ablation targets were determined by pace mapping during sinus rhythm or back up pacing, and/or entrainment mapping during sustained monomorphic VT. Circuit sites of scar-related reentrant VT were defined as exit, central pathway, or entrance sites by determination of the ratio of stimulus to QRS time over VT cycle length (%S-QRS/VT-CL; Exit <30%, Central pathway 30–70%, entrance 70%>) at sites with 12/12 ECG morphology pace-map match to clinical VT, and/or concealed entrainment and post pacing interval minus VT cycle length

<30 msec identified during hemodynamically stable VT.[1–4] If the VT was hemodynamically unstable, the %S-QRS/VT-CL was measured using the S-QRS interval during pacing with the same cycle length as the VT-CL. In addition, VT circuit sites were defined as sites meeting both of the following criteria: a) 11/12 pace-morphology match to the targeted clinical VT, and b) where catheter ablation rendered the VT non-inducible. Additional radiofrequency lesions targeted fractionated and isolated potentials within scar.[1–5, 8–18] Catheter ablation targeting scar or abnormal myocardium adjacent to scar, was performed with maximum power of 50W for 30–60 seconds at each site. When isolated potentials or VT circuit sites as defined above were adjacent (< 1 cm) to a valve annulus or other region of electrically unexcitable scar, lesions were extended to the unexcitable area in the hope of dividing reentry circuit paths as previously described.[9] In such sites, linear RF ablation at 40W was performed until unipolar pacing with an output of 10 mA at 2 ms failed to capture the myocardium. Complete success was defined as noninducibility of any VT. Partial success was defined as suppression of the clinical VT but inducibility of any other VT. In patients with ICD systems devices were reprogrammed to original settings immediately after the procedure.

Registration of EAM Points to LGE-CMR Images

Short axis LGE-CMR image planes were retrospectively registered to the endocardial EAM using previously validated custom software (Volley, Johns Hopkins University) based on the registration coordinates for EAM merge with the LV CMR angiograms.[4,16] Each EAM point was superimposed onto the corresponding sector on short axis LGE-CMR image planes (Figure 1C) and the EGM characteristics corresponding to each image sector were recorded as continuous variables.

Statistical Analysis

Continuous variables are expressed as mean ± SD and categorical data as numbers or percentages. Comparisons of continuous variables were made using the two-group Student's t-test or the Wilcoxon rank-sum test based on the distribution of the values, and categorical variables were compared using the χ^2 or Fisher's exact test where appropriate. Comparisons of continuous variables regarding each EGM parameter were made using ANOVA. Linear mixed effects models, clustered by patient (independent correlation structure), were then used to examine the association of EGM parameters as dependent variables with LV wall thickness, scar transmurality, and intramural scar types (endocardial, mid wall, epicardial, patchy) as independent variables after adjusting for patient gender, age, and left ventricular ejection fraction. Optimal threshold values for bipolar and unipolar voltage, duration and deflection for any nonischemic scar were determined using receiver operating characteristic (ROC) curves. The association of stimulus to QRS time (S-QRS) with scar transmurality was assessed by linear regression. Statistical analyses were performed using STATA software (version 10, StataCorp, College Station, Texas).

Results

Patients Characteristics

A total of 23 patients with nonischemic scar-related VTs were screened. Of the initial 23, 8 patients (34.8%) were excluded due to refusals or screen failures, and the remaining 15 patients (age 51±11 years, 3 female) were included in this study. Five patients had cardiac sarcoidosis and the other 10 patients had idiopathic dilated cardiomyopathy. Other baseline characteristics have been summarized in Table 1. In addition to standard therapy for heart failure, antiarrhythmic drugs (amiodarone and sotalol) had been administrated in 12 patients. Antiarrhythmic drugs were discontinued at least 3 days prior to VT ablation.

Analyzed sectors on LGE-CMR and EAM Points

A total of 2522 image sectors in 113 short axis LGE-CMR image planes and 1957 LV and 752 RV points on EAMs were reviewed. Of 2522 image sectors, 1988 (78.8%) were suitable for quantitative analysis. The remaining 21.2% of image sectors were excluded due to image susceptibility artifacts in patients with ICD systems. Low voltage and dense scar areas defined as <1.5mV and <0.5mV of bipolar voltage covered 8.4% and 1.6% of total LV endocardium on EAM. The mean surface registration error of the LV CMR angiogram with endocardial LV EAM was 2.7±0.4 mm. Ablation procedural details are summarized in Supplemental Table 1. Ablation was not performed in 2 patients because of severe nausea and worsening of heart failure during the procedure, respectively. Figure 2 demonstrates the distribution and characteristics of left ventricular scar in the patient cohort. Nonischemic scars were indentified on 343 (17.3%) of 1988 image sectors (Figure 2A). Patchy scar was identified on 75 (21.9%) of 343 sectors with scar (Figure 2B). Of 334 image sectors with scar, most of the scar was located in basal (55.1%) and mid LV (32.9%) regions.

Comparison of Scar on LGE CMR and EGM characteristics

Univariate comparisons of local EGM and scar features revealed that voltage amplitude was negatively associated with scar transmurality (P<0.0001 by ANOVA for all intramural scar types; Figure 3A, 3B), and that EGM duration and deflections were positively associated with scar transmurality (P<0.0001 by ANOVA for all intramural scar types; Figure 3C, 3D). Of all EAM points analyzed, 4.9% had fractionated EGMs, and 3.3% had isolated potentials. There was a positive association between the incidence of fractionated and isolated potentials with scar transmurality (P<0.0001 by ANOVA for both; Figure 3E) and isolated potentials were more frequently observed in sectors with higher scar transmurality and patchy scar regions (P<0.05 by ANOVA).

Linear mixed effects multivariable model results with EGM parameters as dependent variables and LGE-CMR variables as independent variables, clustered by patient, have been summarized in Table 2. LV wall thickness, scar transmurality, endocardial scar and mid wall scar were independently associated with EGM parameters. Epicardial and patchy scar were also significantly associated with bipolar and unipolar voltage. Unlike epicardial scar, patchy scar was associated with EGM deflections.

The optimal thresholds for identification of nonischemic scar based upon bipolar and unipolar voltage, EGM duration and deflection by ROC curves, and associated sensitivity and specificity measures were: <1.78 mV [sensitivity 79.2%, specificity 88.6%] for bipolar voltage, <5.64mV [69.5%, 86.6%] for unipolar voltage, >101 ms [80.3%, 83.7%] for EGM duration, and >9 [80.5%, 79.9%] for EGM deflection, respectively (Supplemental Figure 1). Supplemental Figure 2 provides optimal thresholds for nonischemic scar identification by intramural scar type.

Comparison of Ablation Sites of Scar-related VT and Scar on LGE-CMR

A total of 98 LV and 78 RV radiofrequency applications were made. Of all lesions in LV endocardium, 22.5%, 37.8%, 18.4%, and 10.2% were delivered to areas with 1–25%, 26–50%, 51–75%, and 76–100% scar transmurality, respectively (Supplemental Figure 3A). Endocardial scar was more frequently targeted than other intramural scar types. Scar regions in the lateral LV (42 sites, 42.9%) and septal RV (40 sites, 39.6%) were more likely to be targeted for ablation (Supplemental Figure 3B, C). Additionally, 11.2% of lesions were delivered to regions without scar on LGE-CMR. Of 11 LV sites without scar on LGE-CMR, 9 were ablated adjacent to scar on LGE-CMR to target abnormal EGMs, guided by pace mapping as well as substrate modification strategies. The remaining 2 sites with normal EGMs were ablated in the same patient to create a linear lesion set connecting two islands of

scar in close proximity (<1 cm). No adverse effects (effusion, decreased EF, or increased heart failure) were observed in these patients. A total of 20 sites of scar-related reentrant VT in the LV (N=12) and RV (N=8) were identified (Figure 4A). Of all VT circuit sites, 5 sites (4 in LV, 1 in RV) were identified as exit sites by both entrainment and pace mapping. The mean VT cycle length was significantly longer in VTs that enabled entrainment mapping, compared to those where only pace mapping was utilized (464±64 vs 314±72ms; P<0.001 by two-group Student's t-test). VT circuit sites were more likely to be identified within endocardial scar (50% in LV and RV septum, respectively; Figure 4B). The mean scar transmurality of VT circuit sites was 39.6±20.7%, and most VT circuit sites were identified in scar with >25% scar transmurality (83.3% in LV, 100% in RV, Figure 4C). In addition, most VT circuit sites were identified in basal (50.0%, 10 sites) and mid regions (35.0%, 7 sites).

Isolated potentials were observed in 3 (15.0%) of 20 VT circuit sites. S-QRS (R=0.482, P=0.047 by Spearman correlation test) and %S-QRS/VT-CL (R=0.500, P=0.046 by Spearman correlation test) were associated with scar transmurality (Figure 4D). Slow conduction defined by >40 msec of S-QRS delay (12.2% of sites), was confined to regions with >75% scar transmurality or patchy scar. In addition, all VT circuit sites demonstrated <30% of %S-QRS/VT-CL and were identified as VT exit sites. Figure 5 provides an example of concealed entrainment during VT, and sinus rhythm local electrograms, from a successful ablation site highlighted on electroanatomic mapping and LGE-CMR.

Comparison of Patient Characteristics between Complete and Partial Success of VT ablation

Table 3 summarizes the characteristics of patients with complete versus partial success. Of 13 patients with reentrant VT ablation, complete success was achieved in 7 and partial success attained in the remaining patients. Patients with complete success were younger {median age of patients with complete success 40 years [interquartile range (IQR) 39–46) versus median age for partial success: 56 (IQR 54–62), Wilcoxon rank-sum test P=0.003] and had less extensive low voltage areas in the right ventricle [complete success: 12.7 cm^2 (IQR 2.6–22) versus partial success 45 cm^2 (IQR 25.3–75), Wilcoxon rank-sum test, P=0.049]. Additionally, the presence of patchy scar was associated with partial success [complete success: 0 sectors (IQR 0–0.5) versus partial success: 3.8 sectors (IQR 1.3–7.5), Wilcoxon rank-sum test P=0.028].

Discussion

The main findings of this study are that a) LV wall thickness, scar transmurality, intramural location, and type, are independently associated with local EGM bipolar and unipolar voltage, duration and deflections; b) most VT exit sites are located in scar regions with >25% scar transmurality; c) sites with evidence of slow conduction are associated with >75% transmurality or patchy scar on LGE-CMR; and d) the presence of extensive regions with patchy scar is associated with incomplete success of VT ablation.

Nonischemic Scar and EGM characteristics

The VT substrate in NICM exhibits more complicated morphology and distribution patterns compared to the substrate in ischemic cardiomyopathy. [19] We noted a preponderance for basal scar distribution consistent with prior reports using voltage mapping in patients with NICM.[8–15] Previous reports have shown associations between ischemic scar on LGE-CMR and local EGMs on EAM.[3–8] However, to the best of our knowledge, aside from a single case report,[16] no clinical studies have previously examined the association of nonischemic scar on LGE-CMR with local EGMs. Psaltis and colleagues demonstrated negative

associations between the extent of scar on LGE-CMR and bipolar and unipolar voltage measures in 12 sheep with NICM induced by doxorubicin coronary infusions.[25] Our results confirm Psaltis and colleagues findings regarding voltage measures in the sheep model. In addition, the present study demonstrated a positive association between scar transmurality and EGM duration and deflections, which suggests the existence of slow conduction in regions with higher scar transmurality regardless of intramural scar distribution. Isolated potentials were associated with regions with higher scar transmurality or patchy scar.

Optimal Thresholds for Scar Identification

Psaltis and colleagues suggested optimal thresholds of 7.5mV for unipolar voltage (sensitivity 77% and specificity 76%) and 2.7mV for bipolar voltage (sensitivity 54% and specificity 76%) for scar identification in their sheep model of NICM.[25] In contrast, Hutchinson and colleagues suggested a unipolar voltage threshold of 8.27mV for detection of scar on endocardial EAM of patients with NICM.[11] Our study is unique in determination of optimal thresholds for identification of nonischemic scar not only for bipolar and unipolar voltage, but also for EGM duration and deflections. Surprisingly, sensitivity and specificity profiles for scar identification using bipolar voltage were relatively high. While the performance of these thresholds is expected to decline with prospective testing, our study suggests that contrary to previous belief, mid wall, epicardial, and patchy scar can be detected by endocardial voltage mapping and EGM duration and deflections.[11,17]

Scar Characteristics on LGE-CMR and VT circuit Sites of Scar-related Reentrant VT

Previous reports have revealed the EGM characteristics of VT circuit sites necessary for VT initiation and maintenance in patients with ischemic[1–5] and NICM.[8–18] In this study, a significant association was observed between circuit site location and regions with 26–75% scar transmurality. Sites in regions with >75% scar transmurality and patchy scar demonstrated >40msec of S-QRS suggesting slow conduction. Additionally, the presence of patchy scar was associated with partial success of VT ablation. In such patients, slow conduction sites may be located epicardially. Consequently, LV endocardial mapping may be limited in the detection of slow conduction sites due to the predilection of nonischemic scar for the midwall and epicardium.

Clinical Implications

Due to atypical nonischemic scar distribution patterns, low voltage areas on endocardial electroanatomic mapping are smaller in patients with nonischemic scar-related VTs than those in patients with ischemic scar-related VTs. In fact, about 50% of the nonischemic scar was located in the mid wall and epicardial LV myocardium, and 75% of scar had less than 50% scar transmurality in this study population. In addition, about 20% of the myocardial sectors on LGE-CMR in patients with nonischemic scar-related VTs contained scar in contrast to 40% of CMR sectors on LGE-CMR in patients with ischemic scar-related VTs.[4] Based upon our findings, endocardial mapping may identify VT exit sites where the target VTs can be eliminated by ablation. Endocardial sites that exhibit slow conduction, correspond to areas with scar transmurality >75% or patchy scar. In addition, if VT circuits within the inter-ventricular septum are suspected in patients with NICM, the RV septum should be mapped. In this study, most ablations were performed using an endocardial approach and successfully suppressed the targeted VTs. However, central VT circuit sites were not identified. It is possible that central circuit sites are predominantly in the mid-wall or epicardium in this population; therefore, if an endocardial approach fails, epicardial access appears warranted

Limitations

The main limitation of this study is the relatively small sample size. Additionally, since the targeted VT was successfully ablated in the majority of patients using an endocardial approach, epicardial mapping was only performed in a subset of patients. Some VT substrates may have been epicardial and missed by endocardial mapping. Further studies will be necessary to confirm our results in larger cohorts with epicardial mapping. In 2 patients ablations were performed adjacent to scar on LGE-CMR to sites with abnormal EGMs or to create a linear lesion set connecting two islands of scar in close proximity. Data regarding the safety and efficacy of this approach is limited.[9] In this study, 16.9% of the sectors on short axis LGE-CMR images were excluded due to MRI susceptibility artifacts from ICD generators.[26] Results may also be limited by a possibility for positional errors when registering EAM points to LGE-CMR images.[3–6, 14, 26] It is important to emphasize that these results are based upon endocardial voltage mapping and the specific LGE-CMR image acquisition parameters specified in the methods section. Therefore, the results are not generalizable to epicardial mapping and other image acquisition protocols. Measurement of EGM duration and deflections may differ depending upon the criteria for analysis. We measured EGM duration and deflections according to the criteria by Tung and colleagues.[23] Inter-observer reliability analysis was not formally performed. However, disagreements among the three observers were rare. Finally, EGM parameters can be affected by mapping catheter contact and orientation.

Conclusions

Strong associations were found between scar characteristics on LGE-CMR and bipolar and unipolar voltage, duration, and deflections on endocardial EAM. These associations suggest that application of optimal thresholds to EGM parameters may improve the detection of nonischemic mid wall, epicardial, and patchy scar. Additionally, VT circuit sites are likely to reside in areas with >25% scar transmurality on LGE-CMR.

Supplementary Material

Refer to Web version on PubMed Central for supplementary material.

Acknowledgments

References

1. Hsia HH, Lin D, Sauer WH, Callans DJ, Marchlinski FE. Anatomic characterization of endocardial substrate for hemodynamically stable reentrant ventricular tachycardia: Identification of endocardial conducting channels. Heart Rhythm. 2006; 3:503–512. [PubMed: 16648052]

2. Stevenson WG, Sager PT, Natterson PD, Saxon LA, Middlekauff HR, Wiener I. Relation of pace mapping QRS configuration and conduction delay to ventricular tachycardia reentry circuits in human infarct scars. J Am Coll Cardiol. 1995; 26:481–488. [PubMed: 7608454]

3. Brunckhorst CB, Stevenson WG, Soejima K, Maisel WH, Delacretaz E, Friedman PL, Ben-Haim SA. Relationship of Slow Conduction Detected by Pace-Mapping to Ventricular Tachycardia Re-Entry Circuit Sties After Infarction. J Am Coll Cardiol. 2003; 41:802–809. [PubMed: 12628726]

4. Sasaki T, Miller CF, Handford R, Yang J, Caffo BS, Zviman MM, Henrickson CA, Marine JE, Spragg D, Cheng A, Tandri H, Sinha S, Kolandaivelu A, Zimmerman SL, Bluemke DA, Tomaselli GF, Berger RD, Calkins H, Halperin HR, Nazarian S. Myocardial Structural Association with Local Electrograms: A Study of Post-infarct Ventricular Tachycardia Pathophysiology and Magnetic Resonance Based Non-Invasive Mapping. Circulation Arrythm Electorphysiol. 2012; 5:1081–1090.

5. Desjardins B, Crawford T, Good E, Oral H, Chugh A, Pelosi F, Morady F, Bogun F. Infarct architecture and characteristics on delayed enhanced magnetic resonance imaging and electroanatomic mapping in patients with postinfarction ventricular arrhythmia. Heart Rhythm. 2009; 6:644–651. [PubMed: 19389653]

6. Codreanu A, Odille F, Aliot E, Marie PY, Magnin-Poull I, Andronache M, Mandry D, Djaballah W, Régent D, Felblinger J, de Chillou C. Electroanatomic characterization of post-infarct scars comparison with 3-dimensional myocardial scar reconstruction based on magnetic resonance imaging. J Am Coll Cardiol. 2008; 52:839–842. [PubMed: 18755347]

7. Perin EC, Silva GV, Sarmento-Leite R, Sousa AL, Howell M, Muthupillai R, Lambert B, Vaughn WK, Flamm SD. Assessing myocardial viability and infarct transmurality with left ventricular electromechanical mapping in patients with stable coronary artery disease: validation by delayed-enhancement magnetic resonance imaging. Circulation. 2002; 106:957–961. [PubMed: 12186800]

8. Nakahara S, Tung R, Ramirez RJ, Michowitz Y, Vaseghi M, Buch E, Gima J, Wiener I, Mahajan A, Boyle NG, Shivkumar K. Characterization of the arrhythmogenic substrate in ischemic and nonischemic cardiomyopathy implications for catheter ablation of hemodynamically unstable ventricular tachycardia. J Am Coll Cardiol. 2010; 55:2355–2365. [PubMed: 20488307]

9. Tokuda M, Tedrow UB, Kojodjojo P, Inada K, Koplan BA, Michaud GF, John RM, Epstein LM, Stevenson WG. Catheter ablation of ventricular tachycardia in nonischemic heart disease. Circ Arrhythm Electrophysiol. 2012; 5:992–1000. [PubMed: 22942218]

10. Cano O, Hutchinson M, Lin D, Garcia F, Zado E, Bala R, Riley M, Cooper J, Dixit S, Gerstenfeld E, Callans D, Marchlinski FE. Electroanatomic substrate and ablation outcome for suspected epicardial ventricular tachycardia in left ventricular nonischemic cardiomyopathy. J Am Coll Cardiol. 2009; 54:799–808. [PubMed: 19695457]

11. Hutchinson MD, Gerstenfeld EP, Desjardins B, Bala R, Riley MP, Garcia FC, Dixit S, Lin D, Tzou WS, Cooper JM, Verdino RJ, Callans DJ, Marchlinski FE. Endocardial unipolar voltage mapping to detect epicardial ventricular tachycardia substrate in patients with nonischemic left ventricular cardiomyopathy. Circ Arrhythm Electrophysiol. 2011; 4:49–55. [PubMed: 21131557]

12. Soejima K, Stevenson WG, Sapp JL, Selwyn AP, Couper G, Epstein LM. Endocardial and epicardial radiofrequency ablation of ventricular tachycardia associated with dilated cardiomyopathy: the importance of low-voltage scars. J Am Coll Cardiol. 2004; 43:1834–1842. [PubMed: 15145109]

13. Hsia HH, Callans DJ, Marchlinski FE. Characterization of endocardial electrophysiological substrate in patients with nonischemic cardiomyopathy and monomorphic ventricular tachycardia. Circulation. 2003; 108:704–710. [PubMed: 12885746]

14. Bogun FM, Desjardins B, Good E, Gupta S, Crawford T, Oral H, Ebinger M, Pelosi F, Chugh A, Jongnarangsin K, Morady F. Delayed-enhanced magnetic resonance imaging in nonischemic cardiomyopathy: utility for identifying the ventricular arrhythmia substrate. J Am Coll Cardiol. 2009; 53:1138–1145. [PubMed: 19324259]

15. Haqqani HM, Tschabrunn CM, Tzou WS, Dixit S, Cooper JM, Riley MP, Lin D, Hutchinson MD, Garcia FC, Bala R, Verdino RJ, Callans DJ, Gsertenfeld EP, Zado ES, Marchlinski FE. Isolated Isolated septal substrate for ventricular tachycardia in nonischemic dilated cardiomyopathy: incidence, characterization, and implications. Heart Rhythm. 2011; 8:1169–1176. [PubMed: 21392586]

16. Sasaki T, Mudd J, Steenbergen C, Zviman MM, Miller CF, Nazarian S. Impact of Scar, Viable Myocardium, and Epicardial Fat on Substrate Identification of Ventricular Tachycardia in a Case with Nonischemic Cardiomyopathy. Pacing Clin Electrophysiol. 2011; 35:345–348.

17. Polin GM, Haqqani H, Tzou W, Hutchinson MD, Garcia FC, Callans DJ, Zado ES, Marchlinski FE. Endocardial unipolar voltage mapping to identify epicardial substrate in arrhythmogenic right ventricular cardiomyopathy/dysplasia. Heart Rhythm. 2011; 8:76–83. [PubMed: 20933099]

18. Jefic D, Joel B, Good E, Morady F, Rosman H, Knight B, Bogun F. Role of radiofrequency catheter ablation of ventricular tachycardia in cardiac sarcoidosis: Report from a multicenter registry. Heart Rhythm. 2009; 6:189–195. [PubMed: 19187909]

19. Karamitsos TD, Francis JM, Myerson S, Selvanayagam JB, Neubauer S. The Role of Cardiovascular Magnetic Resonance Imaging in Heart Failure. J Am Coll Cardiol. 2009; 54:1407–1424. [PubMed: 19796734]

20. Nazarian S, Hansford R, Roguin A, Goldsher D, Zviman MM, Lardo AC, Caffo BS, Frick KD, Kraut MA, Kamel IR, Calkins H, Berger RD, Bluemke DA, Halperin HR. A prospective evaluation of a protocol for magnetic resonance imaging of patients with implanted cardiac devices. Ann Intern Med. 2011; 155:415–424. [PubMed: 21969340]

21. Nazarian S, Bluemke DA, Lardo AC, Zviman MM, Watkins SP, Dickfeld TL, Meininger GR, Roguin A, Calkins H, Tomaselli GF, Weiss RG, Berger RD, Lima JA, Halperin HR. Magnetic resonance assessment of the substrate for inducible ventricular tachycardia in nonischemic cardiomyopathy. Circulation. 2005; 112:2821–2825. [PubMed: 16267255]

22. Harrigan CJ, Peters DC, Gibson CM, Maron BJ, Manning WJ, Maron MS, Appelbaum E. Hypertrophic cardiomyopathy: quantification of late gadolinium enhancement with contrast-enhanced cardiovascular MR imaging. Radiology. 2011; 258:128–133. [PubMed: 21045187]

23. Tung R, Nakahara S, Ramirez R, Lai C, Fishbein MC, Shivkumar K. Distinguishing epicardial fat from scar: Analysis of electrograms using high-density electroanatomic mapping in a novel porcine infarct model. Heart Rhythm. 2010; 7:389–395. [PubMed: 20185114]

24. Vassallo JA, Marchlinski FE, Buxton AE, Untereker WJ, Josephson ME. Endocardial mapping in humans in sinus rhythm with normal left ventricles: activation patterns and characteristics of electrograms. Circulation. 1984; 70:37–42. [PubMed: 6723010]

25. Psaltis PJ, Carbone A, Leong DP, Lau DH, Nelson AJ, Kuchel T, Jantzen T, Manavis J, Williams K, Sanders P, Gronthos S, Zannettino AC, Worthley SG. Assessment of myocardial fibrosis by endoventricular electromechanical mapping in experimental nonischemic cardiomyopathy. Int J Cardiovasc Imaging. 2011; 27:25–37. [PubMed: 20585861]

26. Sasaki T, Hansford R, Zviman MM, e Kolandaivelu A, Bluemke DA, Berger RD, Calkins H, Halperin HR, Nazarian S. Quantitative assessment of artifacts on cardiac magnetic resonance imaging of patients with pacemakers and implantable cardioverter-defibrillators. Circ Cardiovasc Imaging. 2011; 4:662–667. [PubMed: 21946701]
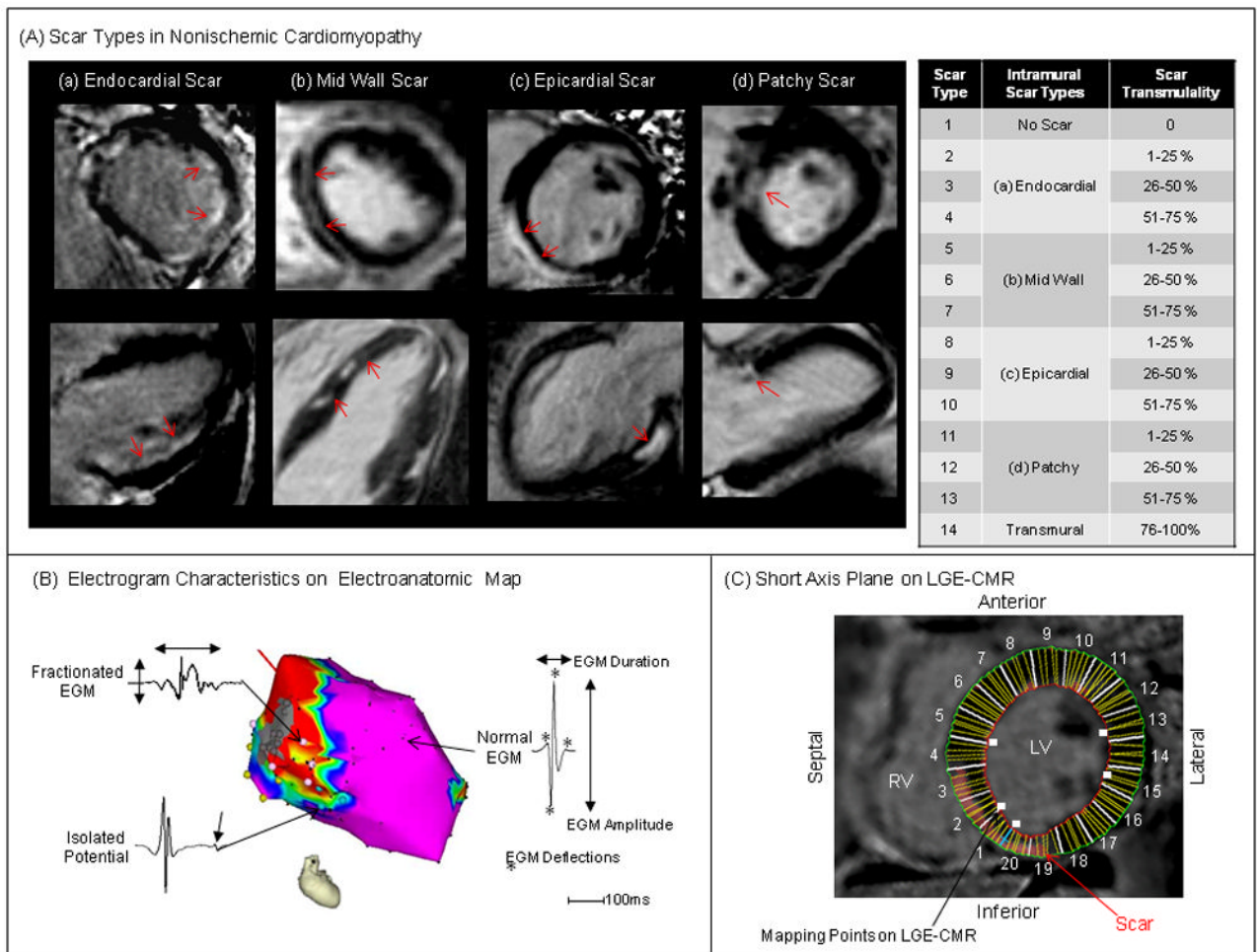
Figure 1.
Scar Types in NICM and Electrogram Characteristics – (A) Scar on LGE-CMR (red arrows) was divided into 14 types by intramural scar types (no scar, endocardial, mid wall, epicardial, patchy, transmural) and scar transmurality (0–25, 26–50, 51–75, 76–100%). The upper right panel shows scar types divided by intramural scar types and scar transmurality. (B) EGM characteristics on EAM were defined as EGM parameters (bipolar and unipolar voltages, duration, deflection) and EGM types (normal, fractionated EGM, isolated potential). (C) Mapping points on EAM were registered to the corresponding region on short axis planes of LGE-CMR.
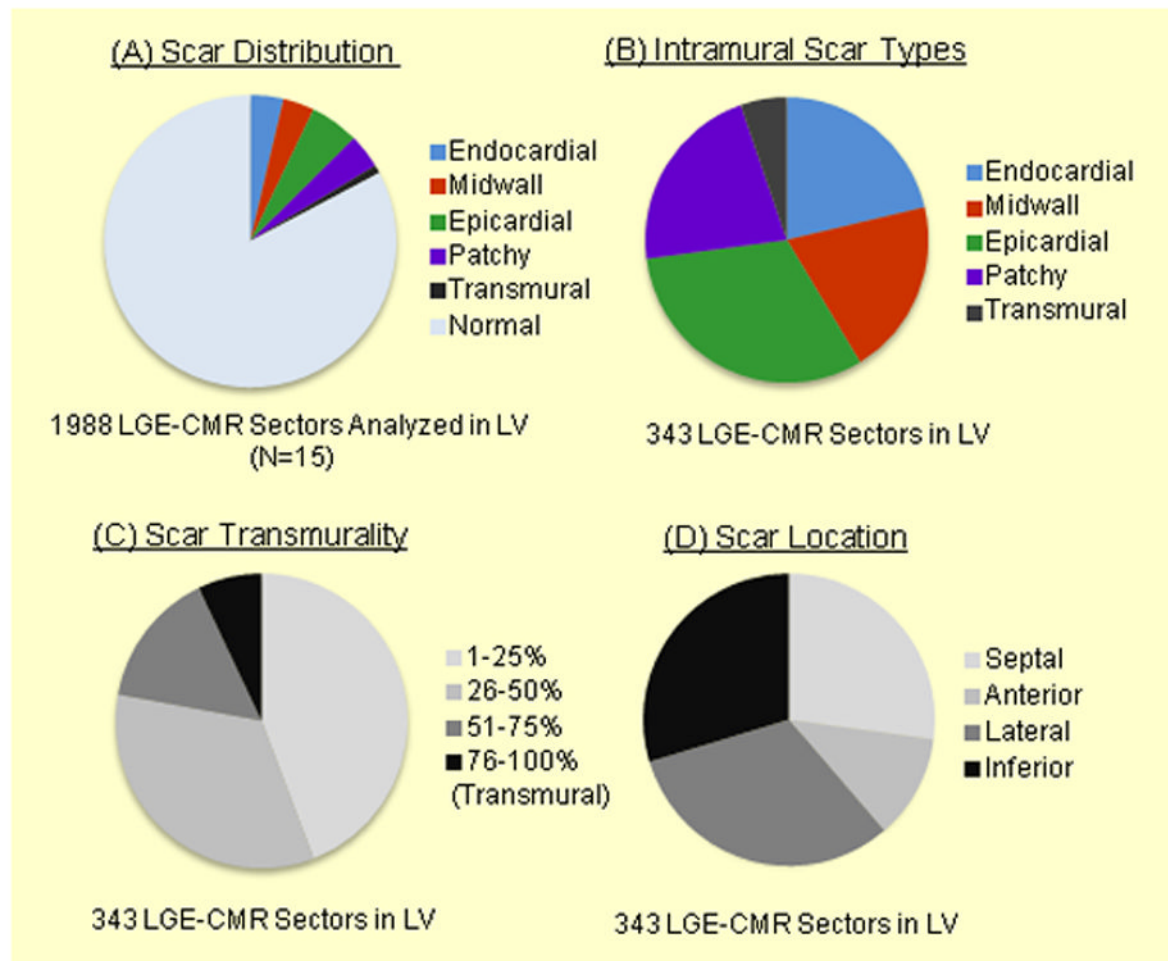
Figure 2.
Scar Characteristics in Patients with Nonischemic VT – The figure illustrates the
distribution (A) and characteristics (B–D) of scar in left ventricle in our patient cohort.
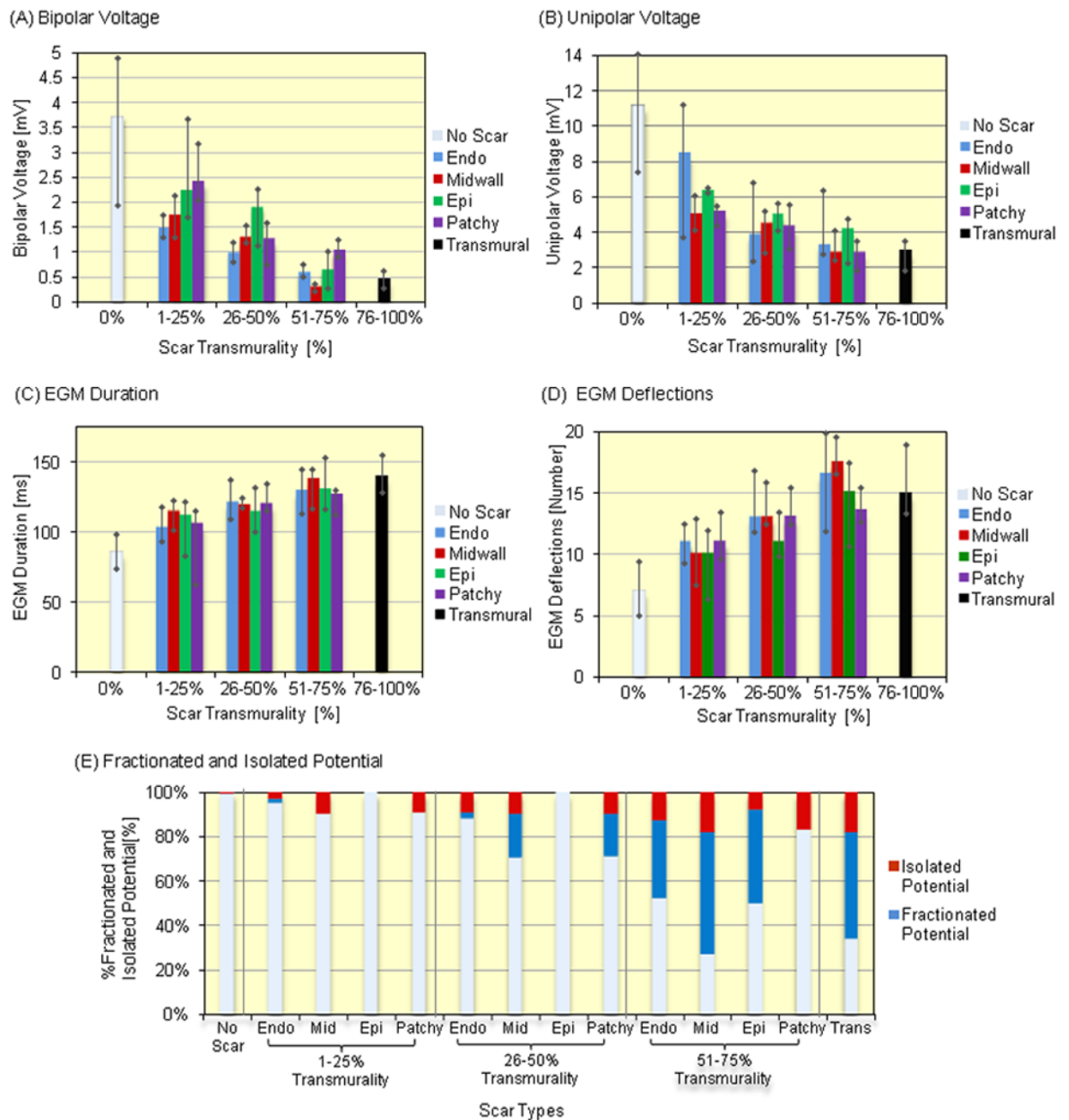
Figure 3.
Associations between Scar on LGE-CMR and Local Electrograms – The figure illustrates the association of EGM parameters or fractionated and isolated potentials with scar types. (A) Bipolar and (B) unipolar EGM voltages were negatively associated with endocardial, mid wall, epicardial and patchy scar transmurality (P<0.0001, respectively, test for trend). (C) EGM duration and (D) deflections were positively associated with endocardial, mid wall, epicardial and patchy scar transmurality (P<0.0001, respectively, test for trend). The bar graphs show the median and the error bars reflect the interquartile range. (E) Fractionated and isolated potential were more frequently observed in scar regions with greater scar transmurality (P<0.0001, test for trend).
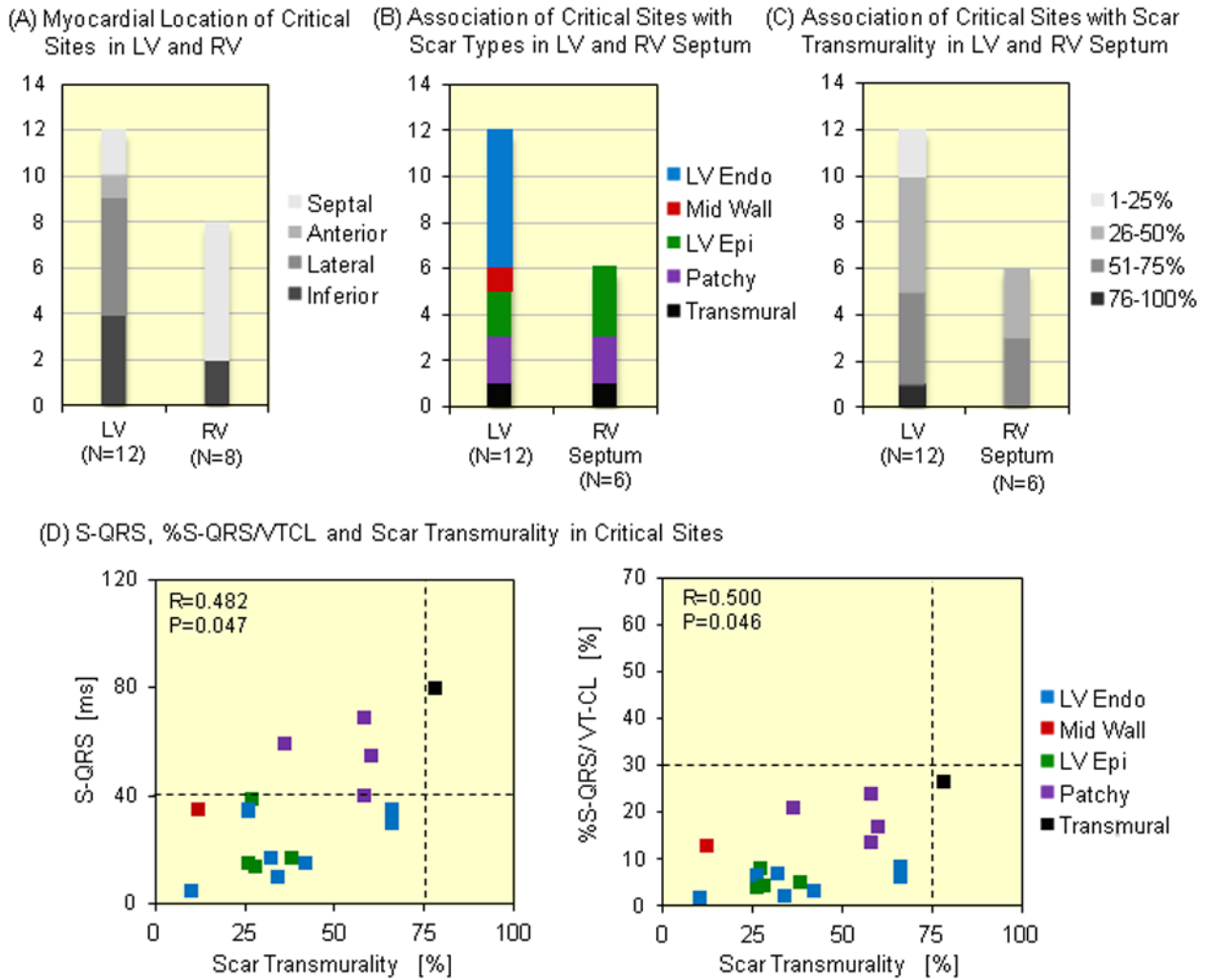
Figure 4.
Associations between Scar on LGE-CMR and VT Circuit Sites of Scar-related VT – A total of 20 VT circuit sites were identified in LV (12 sites) and RV (8 sites) endocardially. (A) The VT circuit sites in LV and RV were more frequently observed in lateral and inferior LV and septal RV regions, respectively. The VT circuit sites were more frequently observed in regions with (B) endocardial scar and (C) 25–75% scar transmurality in LV and RV septum. (D) S-QRS (R=0.482, P=0.047) and %S-QRS/VT-CL (R=0.500, P=0.046) were significantly associated with scar transmurality. The VT circuit sites with 40 ms of S-QRS were associated with 75% scar transmurality and patchy scar.
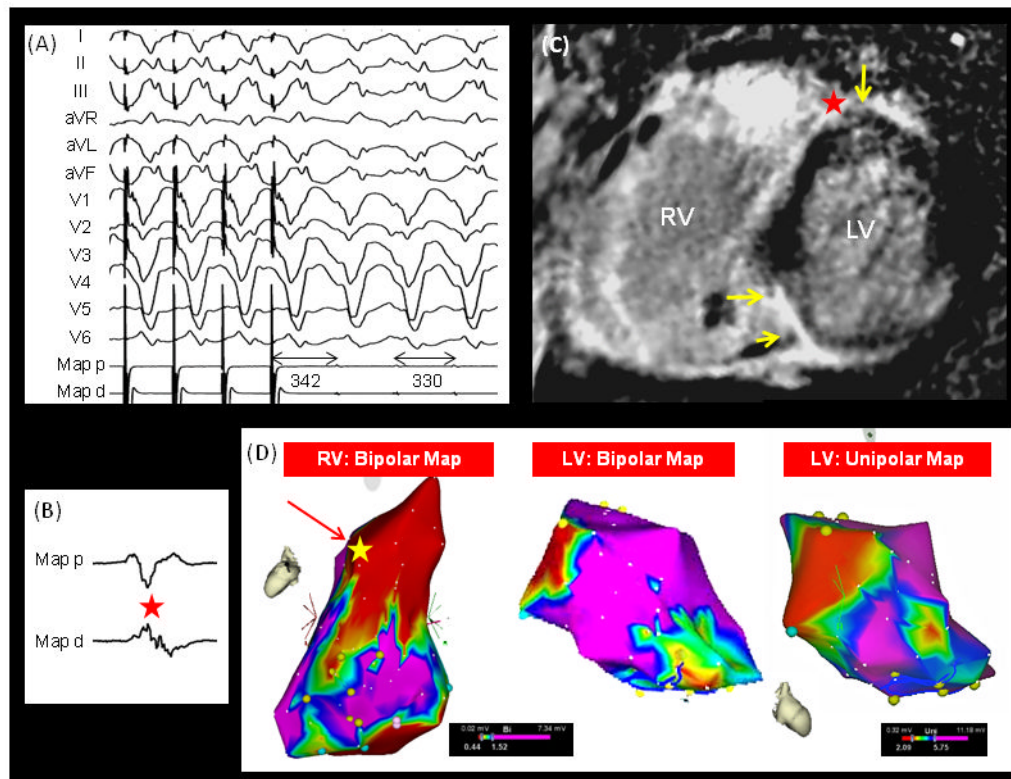
Figure 5.
Successful Ablation Site of a Nonischemic VT on LGE-CMR and Electroanatomic Map – The figure illustrates (A) the 12-Lead ECG shows concealed entrainment with short post pacing interval, (B) local electrograms at the successful ablation site during sinus rhythm, (C) location of the successful ablation site on LGE-CMR (red star), and (D) the successful ablation site on the electroanatomic map (yellow star) in a case with NICM and scar-related VT. The yellow arrows on the LGE-CMR image point to regions of scar.

Table 1

Patient Characteristics

	VT (N=15)
Age [years]	51±11
Gender Male / Female	12 / 3
BMI [kg/m2]	29.4±6.6
Idiopathic / Sarcoidosis	10 / 5
Epicardial Ablation [patients]	2 (13%)
Use of Antiarrhythmic Drug	
Amiodarone / Sotalol / Mexiletine / Flecanide / β Blocker	8 / 3 / 1 / 1 / 9
MRI with In-situ ICD	13
Echocardiography	
Ejection Fraction [%]	41.6±13.0
Left Ventricular Diastolic Diameter [mm]	59.7±13.0
MRI	
LV End-diastolic volume [ml]	154.0±28.5
LV End-systolic volume [ml]	99.0±21.1
LV Stroke Volume [ml/beat]	59.4±22.4
LV Cardiac Output [ml/minute]	4.2±2.3
LV Ejection Fraction [%]	40.6±9.1

Values are expressed as mean ± SD or number. BMI=body mass index; ICD=implantable cardioverter defibrillator; LV=left ventricle.

Table 2

Linear Mixed Effects Multivariable Models

	Electrogram Parameters							
	Bipolar Voltage (mV)		Unipolar Voltage (mV)		Duration (msec)		Deflections (number)	
	B	P	B	P	B	P	B	P
Left Ventricular Wall thickness (mm)	0.327	<0.001*	0.507	<0.001*	−1.542	<0.001*	−0.211	<0.001*
Scar Transmurality (%)	−0.015	0.027*	−0.025	0.005*	0.594	<0.001*	0.630	<0.001*
Endocardial Scar	−1.980	<0.001*	−1.576	0.002*	10.257	0.006*	2.183	<0.001*
Mid Wall Scar	−2.173	<0.001*	−3.040	<0.001*	27.490	<0.001*	2.319	<0.001*
Epicardial Scar	−2.041	<0.001*	−3.944	<0.001*	8.453	0.069	1.012	0.069*
Patchy Scar	−1.297	0.002*	−1.941	0.001*	5.857	0.15	1.544	0.002*
Rhythm During Mapping (Sinus/Atrial Pace, Ventricular Pace, VT)	0.667	0.001*	1.284	<0.001*	−0.623	0.77	0.150	0.52
Gender (Male, Female)	−0.528	0.24	0.672	0.56	12.870	0.088	0.270	0.66
Age (years)	−0.060	<0.001*	−0.132	0.002*	0.443	0.11	0.028	0.18
Left Ventricular Ejection Fraction (%)	0.023	0.048*	0.164	<0.001*	0.213	0.30	−0.043	0.007*
SD of Patient Random Effects	0.222		1.025		6.626		0.410	
SD of Population Residuals	2.642		3.498		23.111		2.731	

Significant regression coefficients and P-values defined as P<0.05 are shown by asterisks (*). B=regression coefficients; P=P-value; SD=standard deviation. See abbreviations in Table 1.

Table 3

Comparisons of Patients Characteristics between the Patients with Complete and Partial Ablation Success

		Complete Success (N=6)	Partial Success (N=7)	P Value
	Male / Female	3 / 3	7 / 0	0.070
	Age	42±4	58±7	0.003*
	Body Mass Index	28.0±5.7	26.4±5.3	0.67
	LV Ejection Fraction	49.1±13.7	44.2±16.0	0.46
	LV End Diastolic Volume	154.9±22.9	153.6±39.6	0.56
	Idiopathic / Sarcoidosis	3 / 3	5 / 2	0.59
	Number of Inducible VT	1.7±0.8	3.3±1.6	0.077
	Number of RF application	17±7	32±14	0.059
	Ablation Location: LV / RV / LV+RV	4 / 2 / 0	4 / 2 / 1	1.0
	Low Voltage Area in LV [cm2]	7.1±10.2	36.0±25.0	0.083
	Low Voltage Area in RV [cm2]	12.4±9.7	48.4±25.0	0.049*
	Total Procedure Time	346±56	443±96	0.063
	Total Ablation Time	12±6	21±15	0.199
	% Sectors with Scar on CMR [%]	12.9±9.1 (119 Sectors)	23.0±10.2 (206 Sectors)	0.116
Intramural Scar Type	Endocardial [%]	2.1±2.5	8.5±7.3	0.072
	Midwall [%]	3.4±2.5	3.4±1.7	0.89
	Epicardial [%]	6.9±5.6	5.1±7.0	0.47
	Patchy [%]	0.5±1.0	5.9±7.8	0.028*
Scar Transmurality	1–25% [%]	7.1±5.3	9.9±3.6	0.25
	26–50% [%]	4.6±3.7	7.4±4.1	0.20
	51–75% [%]	1.1±1.1	3.6±2.4	0.052
	76–100% [%]	0.2±0.5	2.0±2.3	0.062
Scar Location in LV	Septal [%]	4.3±2.9	6.2±4.8	0.31
	Anterior [%]	1.5±2.1	1.4±1.8	0.88
	Lateral [%]	3.4±3.8	6.3±7.4	0.35
	Inferior [%]	3.7±4.6	9.1±6.5	0.086

Values are shown as mean±SD or number. Significant P-values defined as P<0.05 are shown by asterisks (*). LV=left ventricle; RV=right ventricle, CMR=cardiac magnetic resonance.